CONFINING REINFORCEMENT FOR CONCRETE COLUMNS

By S. Watson,[1] F. A. Zahn,[2] and R. Park,[3] Fellow, ASCE

ABSTRACT: Previously derived stress-strain relationships for compressed concrete confined by various quantities and arrangements of transverse reinforcement are used in cyclic moment-curvature analyses of a range of reinforced concrete columns to derive design charts. The design charts permit the enhanced flexural strength of confined columns to be obtained. They also permit the quantities of transverse reinforcement required to achieve particular curvature-ductility factors in the potential plastic-hinge regions of reinforced concrete columns to be determined. The column section is considered to have reached its available ultimate curvature when either the moment resisted has reduced to 80% of the ideal flexural strength, or the strain energy absorbed in the transverse reinforcement has reached its strain energy absorption capacity, or when the logitudinal steel has reached its limiting tensile or compressive strain, whichever occurs first. Refined design equations to determine the quantities of transverse reinforcement required for specified ductility levels are derived on the basis of the design charts. The equations are an improvement on the current provisions of concrete design codes.

INTRODUCTION

Transverse reinforcement in reinforced concrete columns provides confinement to compressed concrete, prevents premature buckling of compressed longitudinal bars, and acts as shear reinforcement. The quantities of transverse reinforcement present in columns designed for seismic resistance should ensure ductile behavior during severe earthquake loading.

In the seismic design of moment resisting frames of buildings it is possible to use a strong column–weak beam approach to reduce the likelihood of plastic hinging in columns during a major earthquake. The extent to which the occurrence of plastic hinges in columns can be eliminated depends on a number of factors, including the ratio of the flexural strength of the columns to that of the beams. In general, it is impracticable to totally eliminate the likelihood of some yielding of columns occurring in moment resisting frames of buildings (Park and Paulay 1975). Also, columns forming part of bridge piers can be deliberately designed to develop plastic hinges during a major earthquake. It is evident that all columns in structures designed for seismic resistance should be detailed for sufficient ductility to sustain the likely inelastic displacements at the design level of seismic loading without significant degradation of strength.

The present paper describes background-research results and an analytical procedure developed to derive refined design charts and equations for the quantities of transverse reinforcement required for concrete confinement to achieve specified ductility levels in the potential plastic-hinge regions of columns. The derived equations more accurately reflect the influence of the significant variables than current code equations. Also, the enhancement of the flexural strength of columns due to confinement by transverse reinforcement is considered. This work is reported in more detail elsewhere (Watson and Park 1989; Zahn et al. 1986).

[1]59 Rountree St., Upper Riccarton, Christchurch, New Zealand; formerly, PhD Student, Dept. of Civ. Engrg., Univ. of Canterbury, Christchurch, New Zealand.

[2]Des. Engr., VSL Int., Ltd., Koenizstrasse 74, CH-3008, Bern, Switzerland.

[3]Prof. and Head of Civ. Engrg., Univ. of Canterbury, Private Bag 4800, Christchurch, New Zealand.

Note. Discussion open until November 1, 1994. Separate discussions should be submitted for the individual papers in this symposium. To extend the closing date one month, a written request must be filed with the ASCE Manager of Journals. The manuscript for this paper was submitted for review and possible publication on March 27, 1992. This paper is part of the ***Journal of Structural Engineering***, Vol. 120, No. 6, June, 1994. ©ASCE, ISSN 0733-9445/94/0006-1798/$2.00 + $.25 per page. Paper No. 3687.

ACI AND NEW ZEALAND CODE EQUATIONS

The special provisions for seismic design in Chapter 21 of ACI 318-89 and the sesmic design provisions of the New Zealand Concrete Design Code (NZS 3101) give equations for the design of transverse reinforcement for the confinement of columns in potential plastic-hinge regions. The ACI code equations are based mainly on a philosophy of preserving the ultimate load-carrying capacity of concentrically loaded columns after spalling of the cover concrete, rather than emphasizing the required ultimate curvature deformation of eccentrically loaded columns. The New Zealand code equations are based on earlier Structural Engineer Association of California (SEAOC) equations ("Recommended lateral forces" 1975), but have a New Zealand derived modification factor that takes into account the influence of the level of axial compressive load on the available ultimate curvature of columns. That modification factor was found from theoretical monotonic moment-curvature analyses (Park and Sampson 1972; Park and Norton 1974; Park and Leslie 1977) using conservative stress-strain curves for confined concrete.

REFINED APPROACH BASED ON MOMENT-CURVATURE ANALYSIS

Approach

The logical approach for the determination of the quantity of confining reinforcement required in the potential plastic-hinge region of a column is to ensure that the column section has a satisfactory cyclic moment-curvature relationship up to the desired level of ultimate curvature. In a refined analysis, included as variables would be the level of axial compressive load on the section, the longitudinal-reinforcement ratio, the cyclic stress-strain relationship for the longitudinal reinforcement, and the cyclic stress-strain relationships of the cover concrete and of the confined core concrete as a function of the transverse reinforcement. A difficulty with such analyses in the past has been the lack of comprehensive data on the cyclic stress-strain relationships for concrete confined by various arrangements of transverse reinforcement. In recent years, however, a great deal of laboratory research has been conducted in many countries that has resulted in a better understanding of the stress-strain behavior of confined concrete. The research in New Zealand has been summarized elsewhere (Priestley and Park 1984, 1987; Park and Paulay 1990).

Stress-Strain Model for Confined Concrete

Mander et al. (1984, 1988a, 1988b) analyzed the results of concentric load tests conducted on large reinforced concrete columns confined by either spirals or circular hoops, or by rectangular hoops with or without cross ties. Typical results are idealized in Fig. 1, which compares the longitudinal stress-strain curve of well-confined concrete with the curve for identical, but unconfined concrete. The passive lateral confining pressure exerted by the transverse reinforcement on the core concrete when the transverse strains

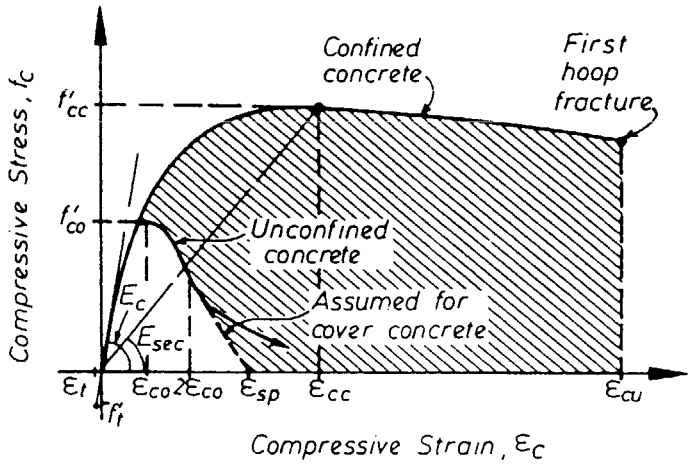

FIG. 1. Concrete Compressive Stress-Strain Model Proposed by Mander et al. (1984, 1988a, 1988b)

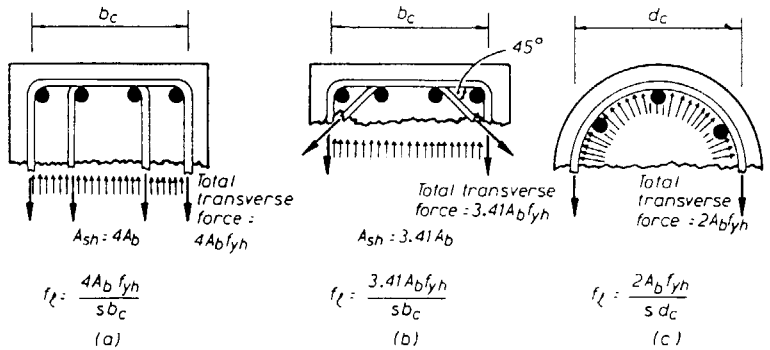

FIG. 2. Confining Stresses Provided by Different Arrangements of Transverse Reinforcement

in the concrete become significant results in the core concrete being placed in a state of triaxial compression, thus enhancing the compression strength and causing a more ductile post-peak stress-strain behavior. Eventual fracture of the transverse reinforcement limits the useful ultimate longitudinal compression strain of the confined concrete. However, for volumetric ratios of transverse reinforcement typical of well-confined columns designed according to seismic design codes, longitudinal compression strains of the confined concrete in the range of 0.02–0.08 at the stage of fracture of the transverse reinforcement are generally obtained.

Mander et al. (1984, 1988a, 1988b) have developed a model for the stress-strain curve of confined concrete based on experimental results. In the model, the effective lateral confining stress in each direction, exerted on the concrete core by the transverse reinforcement at the yield strength, is given by

$$f'_l = k_e f_l \tag{1}$$

where f_l is the confining stress calculated as in Fig. 2 and k_e is a confinement

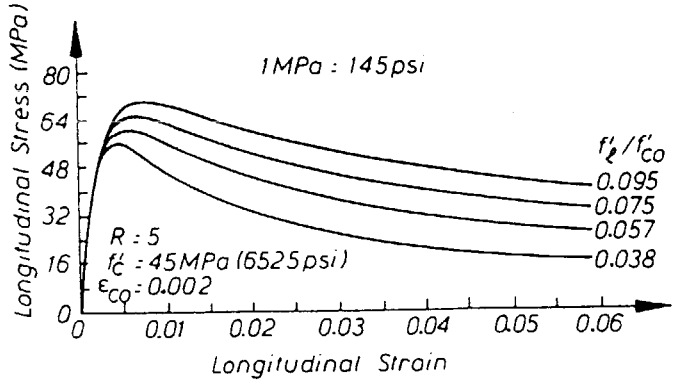

FIG. 3. Stress-Strain Curves Given by Mander et al. (1984, 1988a, 1988b) for Spirally Confined Concrete with Various Levels of Effective Lateral Confining Stress

effectiveness coefficient that takes into account the arching of the concrete between the transverse and longitudinal reinforcement. The coefficient k_e was defined by Mander et al. (1984, 1988a, 1988b) as the ratio of the area of effectively confined core concrete to the area of concrete within the centerlines of the peripheral hoop or spiral. For sections with equal effective lateral confining stress in each direction, the ratio of the compressive strength of the confined concrete f'_{cc} to the compressive strength of unconfined concrete f'_{co} is given by

$$\frac{f'_{cc}}{f'_{co}} = 2.25\sqrt{1 + 7.94\frac{f'_l}{f'_{co}}} - 2.0\frac{f'_l}{f'_{co}} - 1.25 \tag{2}$$

Fig. 3 shows examples of stress-strain curves given by the model for spirally confined concrete with various levels of effective lateral confining stress.

Stress and strain at the peak stress for confined concrete (f'_{cc}, ε_{cc}) and at the peak stress for unconfined concrete (f'_{co}, ε_{co}) in the model are related by the parameter

$$R = \frac{\frac{\varepsilon_{cc}}{\varepsilon_{co}} - 1}{\frac{f'_{cc}}{f'_{co}} - 1} \tag{3}$$

where R = an experimentally determined value (Mander et al. 1984, 1988a, 1988b). Strain rate is taken into account in the model by using values for the control parameters f'_{co}, ε_{co} and the modulus of elasticity of the concrete E_c, which correspond to the relevant strain rate.

Relationships for the cyclic stress-strain behavior of concrete are also given by the model. It is assumed that the monotonic stress-strain curve forms an envelope for the cyclic stress-strain branches. Fig. 4 shows typical stress-strain curves for cyclic compressive loading in the inelastic range.

Ultimate Concrete Compressive Strain

The ultimate longitudinal concrete compressive strain of confined concrete is defined in the present study as the longitudinal strain when the

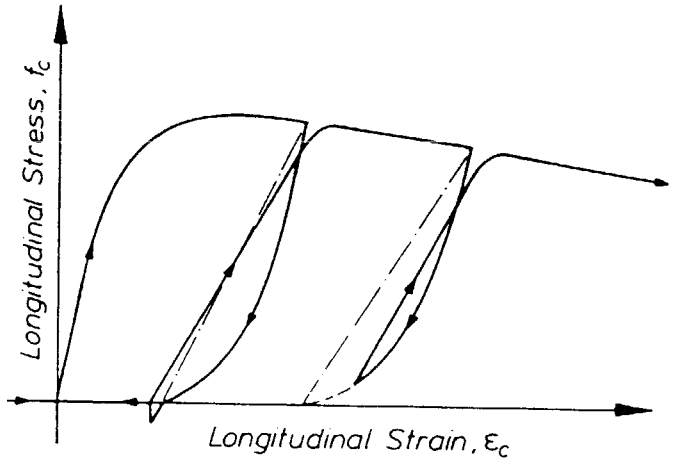

FIG. 4. Cyclic Compressive Stress-Strain Behavior of Confined Concrete

transverse reinforcement first fractures, since that event results in a sudden reduction in the confinement of the concrete. Mander et al. (1984, 1988a, 1988b) have proposed an energy-balance method to predict the longitudinal concrete compressive strain at the stage of fracture of the transverse reinforcement. The energy-balance method reflects the principle that the lateral expansion of the core concrete at large compression strains is passively resisted by the confining steel, which has to follow that expansion, thus absorbing strain energy. The increase in strain energy capacity of the compressed concrete due to confinement is assumed to be provided by the strain-energy capacity of the transverse reinforcement.

The ultimate longitudinal concrete compressive strain is calculated by equating the strain energy stored in the transverse reinforcement at fracture to the sum of the strain energy stored in the concrete as a result of the confinement (given by the shaded area of Fig. 1 multiplied by the volume of confined concrete) and the strain energy required to maintain the yield of the longitudinal reinforcement. If the strain energy accumulated in a hoop or spiral bar over a number of curvature cycles in the inelastic range has reached the strain-energy absorption capacity of the transverse bar, causing it to fracture, the section may be considered to be at an ultimate limit state, since the concrete is no longer effectively confined.

Stress-Strain Model for Steel Reinforcement

Stress-strain curves for typical reinforcing steel measured during monotonic loading tests, such as shown in Fig. 5, can be idealized into an elastic region, a yield plateau, and a strain-hardening region, as shown in Fig. 6.

Mander et al. (1984) found that the stress-strain curve in the strain hardening region ($\varepsilon_{sh} \le \varepsilon_s \le \varepsilon_{su}$) can be predicted with good accuracy by

$$f_s = f_{su} - (f_{su} - f_y)\left(\frac{\varepsilon_{su} - \varepsilon_s}{\varepsilon_{su} - \varepsilon_{sh}}\right)^P \tag{4}$$

where ε_s = steel strain; ε_{sh} = steel strain at commencement of strain hardening; ε_{su} = steel strain at f_{su}; f_s = steel stress; f_{su} = ultimate tensile strength

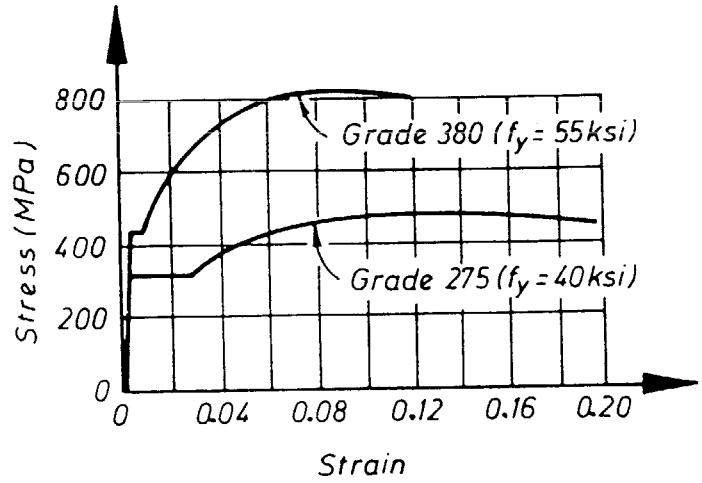

FIG. 5. Typical Stress-Strain Curves for Steel Reinforcement

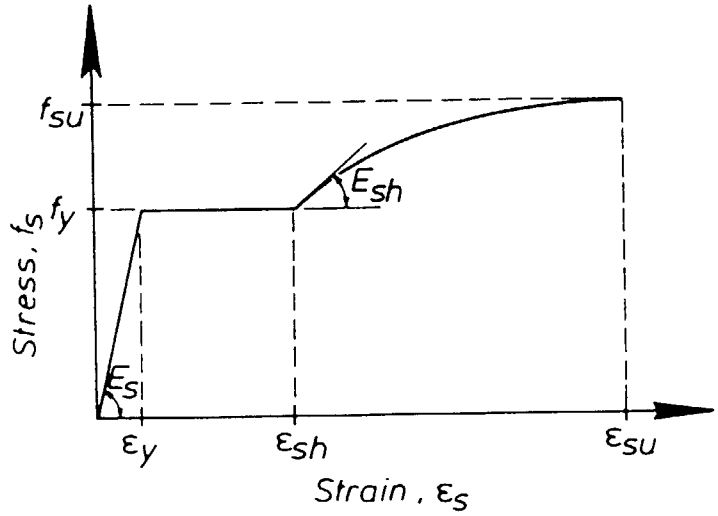

FIG. 6. Steel Stress-Strain Model

of steel; f_y = yield strength of steel; E_{sh} = strain-hardening modulus of steel; and

$$P = E_{sh}\left(\frac{\varepsilon_{su} - \varepsilon_{sh}}{f_{su} - f_y}\right) \tag{5}$$

Strain rate is taken into account by using values for the control parameters that correspond to the relevant strain rate.

Mander et al. (1984) have also proposed a general model for predicting the cyclic stress-strain behavior illustrated in Fig. 7, for various grades of reinforcing steel at any strain level. Envelopes of stress-strain behavior are

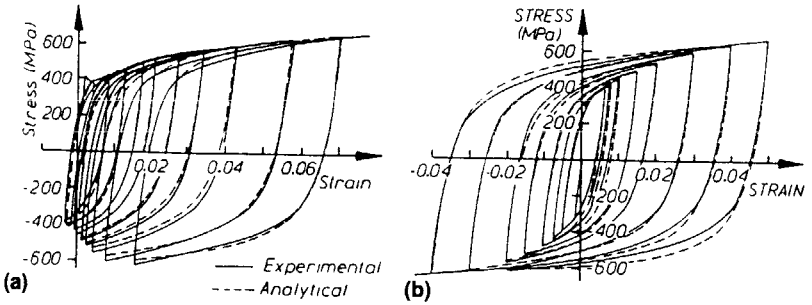

FIG. 7. Experimental and Theoretical Stress-Strain Curves for Grade 380 [f_y = 380 MPa (55 ksi)] Reinforcing Steel (Mander et al. 1984): (*a*) with Unsymmetrical Strain Cycles; (*b*) with Symmetrical Strain Cycles

provided by a skeleton branch curve identical to the monotonic stress-strain relationship. To cope with the inelastic cyclic behavior illustrated in Fig. 7(*a*), it is necessary to shift the strain origin to account for previous inelastic excursions. Fig. 7 shows some experimental curves compared with the analytical predictions.

Moment-Curvature Analysis

Theoretical cyclic moment-curvature relationships for reinforced concrete-column sections can be calculated using well-known theory (Park and Paulay 1975), which assumes that plane sections before bending remain plane after bending. In the present study, the stress-strain relations for confined and unconfined concrete developed by Mander et al. (1984, 1988a, 1988b) were used to determine the compressive stress distribution in the core concrete and the cover concrete, respectively, for a given extreme fiber compression strain. The cover concrete is assumed to cease carrying a load when the spalling strain ε_{sp} is reached (see Fig.1).

To compute the moment-curvature relationship for a given column section and axial-load level, it is convenient to divide the section into a number of discrete laminae, each having the orientation of the neutral axis (Park and Paulay 1975). The longitudinal steel reinforcement may be replaced by an equivalent thin tube with equivalent wall thickness to give the same total area of longitudinal reinforcement, or considered as a discrete number of bars of reinforcing steel. Fig. 8 shows the idealization of a square section. Note that the concrete laminae each contain an area of core concrete and cover concrete, for which different stress-strain relations apply as earlier. A similar approach is used for circular sections. The stress-strain model for the longitudinal steel derived by Mander et al. (1984) was used in the present study. The moment-curvature relationships for a column section can be traced by increasing the extreme fiber concrete compression strain and satisfying the equilibrium conditions.

The energy-balance approach can be used to calculate the stage of first fracture of the transverse reinforcement. However, the value of the ultimate longitudinal concrete compression strain when first fracture occurs for a column section under eccentric loading exceeds the value predicted for concentric loading. This is because the area of concrete subjected to compression stress is normally less than the full core area, and the average strain over the compression stress block is only a half of the maximum. Consequently, for a given extreme fiber compression strain, the strain energy required to deform the core concrete is substantially less in the case of eccentric compression than for concentric compression. Conversely, for a given amount of available strain energy (equal to the capacity of the transverse steel), a higher extreme fiber concrete compression strain can be obtained in the case of eccentric compression than of concentric compression. These considerations were included in the energy-balance approach used in the present study.

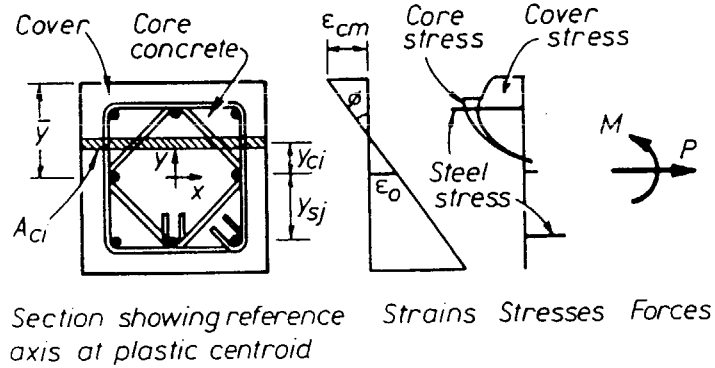

FIG. 8. Moment-Curvature Analysis of a Reinforced Concrete-Column Section

DESIGN CHARTS FOR FLEXURAL STRENGTH AND DUCTILITY

Cyclic Moment-Curvature Analysis

A computer program for cyclic moment-curvature analysis developed by Mander et al. (1984) was used by Zahn et al. (1986a) to derive design charts for the flexural strength and ductility of reinforced concrete columns.

Comparison with experimental results demonstrated that the peaks of the experimental moment-curvature loops for column sections with reasonably low axial compression-load levels could be predicted reasonably well by a simple monotonic moment-curvature analysis using monotonic stress-strain models for the steel and the concrete, providing that bar buckling did not cause additional strength degradation that was not accounted for in the analysis. However, when the axial compression load level was high, a significant moment deterioration at large curvatures with cyclic loading appeared to make monotonic moment-curvature analysis unconservative. Hence, it was decided to use cyclic moment-curvature theory in the derivation of the design charts (Zahn et al. 1986a).

Definition of Ultimate Curvature

A sequence of four identical cycles of imposed bending moment, to peak curvatures of equal magnitude in both the positive and negative directions, was adopted as the standard by which the available curvature-ductility factor of reinforced concrete-column sections could be measured in seismic design.

The column section is considered to have reached its available ultimate curvature when one of the following limit conditions is reached:

1. The moment resisted at either the positive or negative peak of the last cycle has reduced to $0.8M_i$, where M_i = ideal flexural strength of the section.
2. The strain energy accumulated in the transverse steel at the end of the four cycles has become equal to its strain-energy absorption capacity.

3. The tensile strain in the longitudinal reinforcing steel has exceeded ε_{su}, where ε_{su} = strain at the ultimate tensile strength.
4. The compression strain in the longitudinal compression steel has exceeded ε_{suc}, where ε_{suc} = strain when significant inelastic buckling occurs.

The curvature at the first of these four limit conditions to be reached is defined as the available ultimate curvature ϕ_u.

For limit condition 4, the limiting compression strain in the steel reinforcement ε_{suc} can be shown to be a function of the s/d_b ratio, where s = center-to-center spacing of transverse reinforcement along the longitudinal bar; and d_b = diameter of the longitudinal bar. Values for ε_{suc} were derived by Zahn et al. (1986). The buckling model illustrated in Fig. 9 was used and it was derived that

$$\frac{s}{d_b} = 1.5\sqrt{\frac{E_r}{f_{suc}}} \tag{6}$$

where E_r = reduced modulus; and f_{suc} = buckling stress. The value s/d_b required to control bar buckling can be obtained from (6) given the stress-strain curve for the steel and either the compressive strain ε_{suc} or compressive stress f_{suc} at buckling. Fig. 10 shows the result for a typical batch of Grade 380 [f_y = 380 MPa = 55 ksi] deformed steel bars (manufactured by Pacific Steel, Ltd., Auckland, New Zealand) calculated by Zahn et al. (1986a) using the monotonic stress-strain relation for the steel. Two cases are plotted in Fig. 10. For case 1, the specified yield strength, average ultimate tensile strength, and average strain-hardening modulus were used. For case 2, the

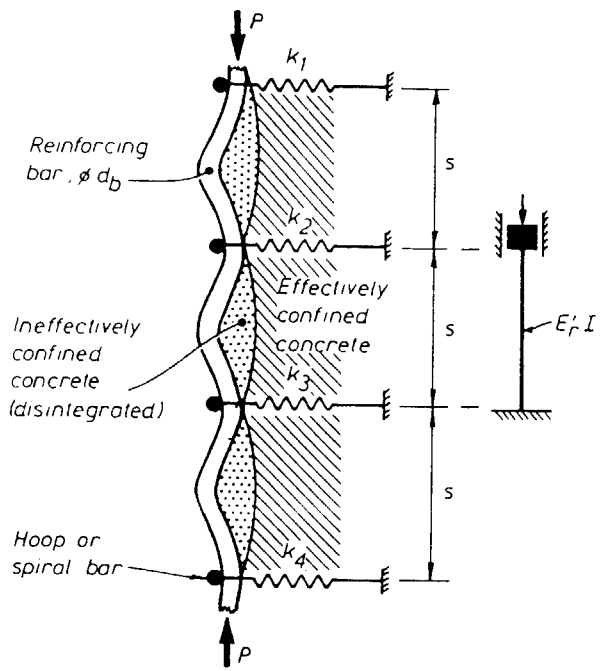

FIG. 9. Model for Buckling of Compression Reinforcement

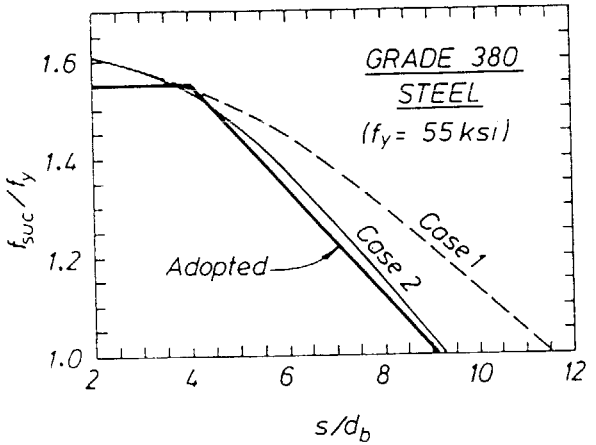

FIG. 10. Ratio of Theoretical Buckling Stress to Yield Strength for Typical Steel Reinforcing Bar (Zahn et al. 1986a).

average yield strength, average ultimate tensile strength, and lowest strain-hardening modulus were used. The curve used for limit condition 4 in this column analysis is also shown in Fig. 10.

It was found in the analysis that limit condition 3 was not critical, and, for close spacing of transverse reinforcement, limit condition 4 did not govern. Thus, limit conditions 1 and 2 were used to define the available ultimate curvature. These two limit conditions are illustrated in Figs. 11 and 12. For the column section in Fig. 11, the available ultimate curvature ϕ_u is governed by moment deterioration to $0.8M_i$ at the end of four cycles to $\pm\phi_u$ without fracture of the hoop steel occurring. For the column section in Fig. 12, the available ultimate curvature is governed by hoop fracture at the end of four cycles to $\pm\phi_u$, without the moment reducing to $0.8M_i$.

It is not known before the analysis commences whether four cycles to a particular curvature peak ϕ_{peak} actually produce an ultimate limit state as defined previously. However, the available ultimate curvature can be determined by an iterative process. The section is analyzed for the standard sequence of four cycles to a first estimate of ϕ_{peak}. If an ultimate limit condition is not reached, the entire cyclic analysis is repeated for improved estimates of ϕ_{peak} until an ultimate limit-state condition is reached, indicating that the final value of ϕ_{peak} is equal to the available ultimate curvature ϕ_u.

In these moment-curvature analyses, no explicit limitation was imposed on the maximum concrete compression strain. Some previous definitions for available ultimate curvature have included a limit on the concrete compression strain. However, it is considered that the limit conditions described give an improved measure of the available ultimate curvature of the section. Numerous column tests have shown that very high compressive strains are tolerated by well-confined concrete [e.g., Priestley and Park (1984, 1987); Mander et al. (1984, 1988a, 1988b); Zahn et al. (1986a)].

Definition of Ideal Flexural Strength and Maximum Moment

In Figs. 11 and 12, M_i is the ideal flexural strength and M_{max} is the maximum moment resisted during the four cycles. Note that M_{max} could occur anywhere along the hysteresis loops, for example at one of the curvature peaks.

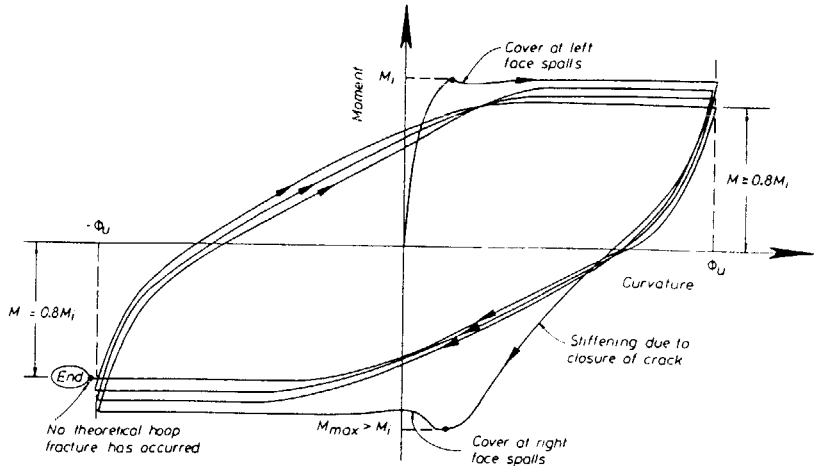

FIG. 11. Theoretical Moment-Curvature Relation for Reinforced Concrete-Column Section Illustrating Case Where Moment Deterioration Governs Available Ultimate Curvature

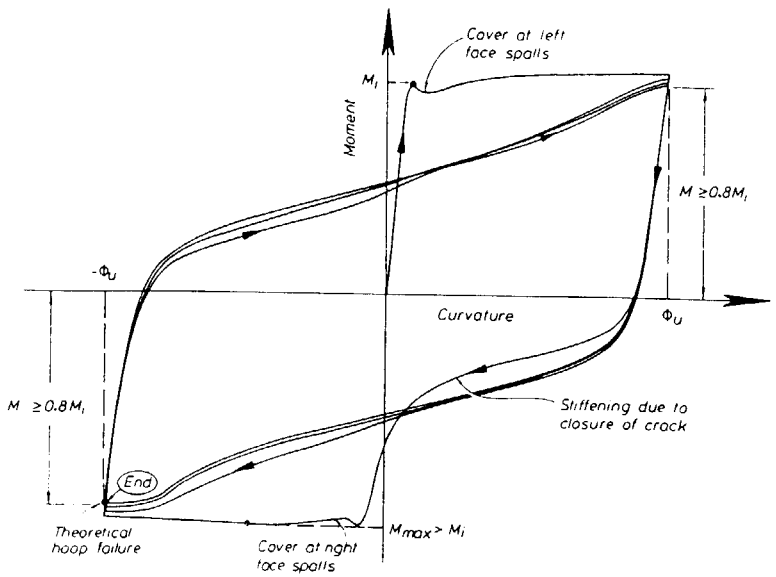

FIG. 12. Theoretical Moment-Curvature Relation for Reinforced Concrete-Column Section Illustrating Case Where Hoop Fracture Governs Available Ultimate Curvature

In the present study, the ideal flexural strength M_i is defined as the maximum moment reached in the initial (positive) half cycle before the curvature at the section exceeds $5\phi_y$, where ϕ_y = yield curvature. Two different cases are illustrated in Fig. 13. In case 1, the moment drops after the spalling of the cover concrete and rises only very slowly (due to strain hardening of the tensile steel) with further increase in curvature, so that at

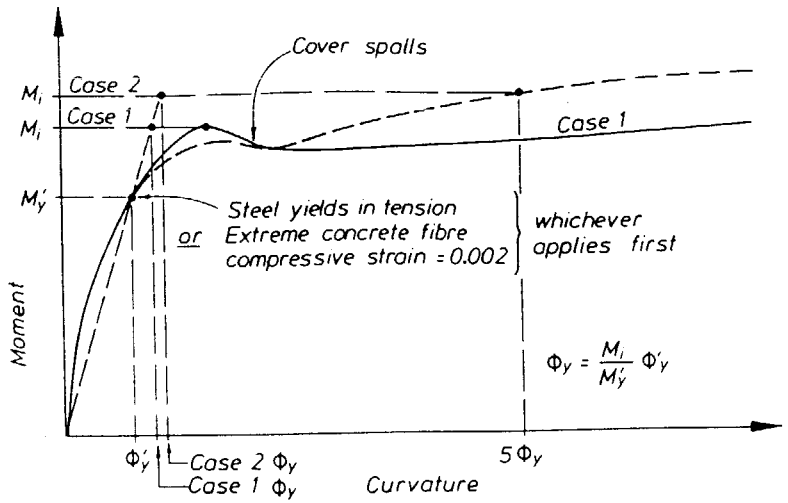

FIG. 13. Definitions of Ideal Moment and Yield Curvature

a curvature of $5\phi_y$ the moment has not regained the maximum value attained before the spalling of the cover concrete. In that case, M_i, is given by that maximum moment. Case 1 is typical for columns with a low axial load and/or a relatively small amount of transverse steel. Also, columns with a relatively large thickness of cover concrete are likely to belong to that category. Case 2, on the other hand, is typical for columns with a relatively small thickness of concrete cover, with a high axial load, and that are heavily confined. The spalling of the cover concrete makes little difference to the resisting moment, so that it rises considerably after spalling of the cover concrete. M_i is then assumed to be given by the moment calculated when the curvature has reached $5\phi_y$.

Definition of Yield Curvature

The yield curvature ϕ_y is defined, as shown in Fig. 13, by the extrapolation of the straight line joining the origin with the point (ϕ'_y, M'_y), so that

$$\phi_y = \frac{\phi'_y M_i}{M'_y} \tag{7}$$

where ϕ'_y and M'_y = curvature and the corresponding moment calculated at the instant when the steel closest to the tension face of the section is yielding or when the extreme fiber concrete compression strain reaches 0.002, whichever applies first. This dual definition of the first-yield point was preferred to the conventional steel-yielding criterion, because in columns with high axial loads the tension steel normally does not yield before the section has lost a considerable percentage of the flexural stiffness.

Material Properties Assumed in Design Charts

The compressive strength of unconfined concrete in columns f'_{co} was assumed to be 85% of the cylinder strength f'_c. This reduction reflects the scale effects observed when comparing the compressive strength of test cylinders with that of large-size cast in place columns. In the cyclic stress-strain model for concrete of Mander et al. (1984, 1988a, 1988b), it was

TABLE 1. Assumed Values for Parameters of Skeleton Curve for Steel Reinforcement

Property (1)	Grade 275 Steel		Grade 380 Steel	
	Tension curve (2)	Compression curve (3)	Tension curve (4)	Compression curve (5)
f_y (MPa)	275	275	380	380
f_{su} (MPa)	420	400	615	590
ε_{sh}	0.022	0.012	0.010	0.006
ε_{su}[a]	0.20	0.070	0.15	0.060
E_s (MPa)	204,000	204,000	204,000	204,000
E_{sh} (MPa)	4,900	6,860	8,800	12,320

[a]Strain at peak stress f_{su} and not the fracture strain (1 MPa = 145 psi).

assumed that $\varepsilon_{co} = 0.002$, $\varepsilon_{sp} = 0.005$ for the cover concrete, $R = 5$, $E_c = 5{,}000\sqrt{f'_c}$ MPa, and $f'_t = 0.6\sqrt{f'_c}$ MPa, where ε_{sp} = compressive strain in cover concrete when spalling occurs (see Fig. 1) and f'_t = modulus of rupture of concrete. Also, $k_e = 0.85$ for spirals or circular hoops, and $k_e = 0.70$ for rectangular hoops were assumed.

In the cyclic stress-strain model for steel of Mander et al. (1984), the parameters shown in Table 1 were assumed for the skeleton curve (Fig. 6). These were based on average values measured in research projects at the University of Canterbury in recent years.

Design Charts to Determine Curvature-Ductility Factor

Fig. 14 shows an example of the curvature-ductility design charts derived by Zahn et al. (1986a) for circular reinforced concrete-column sections. The chart relates the available curvature-ductility factor ϕ_u/ϕ_y at the critical section of the plastic hinge to the magnitude of the effective lateral confining stress f'_l acting on the core concrete and the axial load level P/f'_cA_g, where P = axial compressive load in column; and A_g = gross area of column.

Charts were derived for a range of column properties. The chart shown in Fig. 14 is for a circular section with $f'_c = 30$ MPa (4.35 ksi), $f_y = f_{yh} = 275$ MPa (40 ksi), and mechanical reinforcing ratios of $\rho_t m = 0.1$ and 0.2, where ρ_t = ratio of area of longitudinal steel to gross area of column and $m = f_y/0.85f'_c$. The thickness of the unconfined cover concrete of the section is 6% of the overall section diameter.

The charts allow the designer to determine the effective lateral confining stress f'_l required for a given reinforced concrete-column section, axial load, and curvature-ductility factor demand. From the obtained effective lateral confining stress necessary for a particular situation, it is then possible to determine the quantity of transverse spiral or hoop steel necessary to provide that confinement.

From Fig. 14 and other charts, the following general conclusions can be reached:

- The available curvature-ductility factor ϕ_u/ϕ_y of columns rapidly decreases with increasing axial-load ratio P/f'_cA_g.
- At low axial-load ratios (<0.15) extremely large curvature-ductility factors are available with only very small quantities of confining steel. In such cases, the amount of transverse reinforcement required is not governed by the requirements of concrete confinement.
- The factor that most often governs the ultimate curvature of the section is the cyclic flexural-strength deterioration, as indicated by the "○" symbols in Fig. 14.
- The available curvature-ductility factor for a given confining stress ratio f'_l/f'_{co} is greater for higher mechanical reinforcing ratios $\rho_t m$.

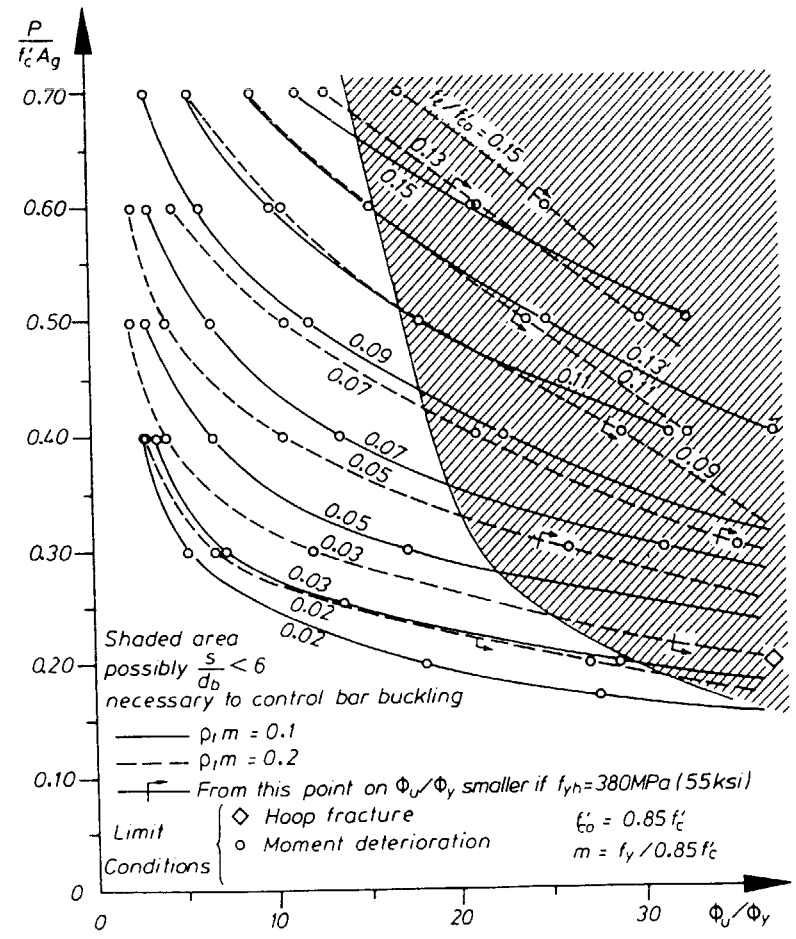

FIG. 14. Design Chart for Curvature-Ductility Factor for Circular Reinforced Concrete-Column Sections

Design Charts to Determine Flexural Strength

Fig. 15 shows an example of charts derived by Zahn et al. (1986) to determine the ideal flexural strength of a circular column with $\rho_t m = 0.1$, $f_y = 275$ MPa (40 ksi), and f'_c anywhere in the range from 20 MPa (2,900 psi) to 40 MPa (5,800 psi). The chart gives the ratio M_i/M_{code} where M_i = ideal flexural strength taking into account the increase in strength due to

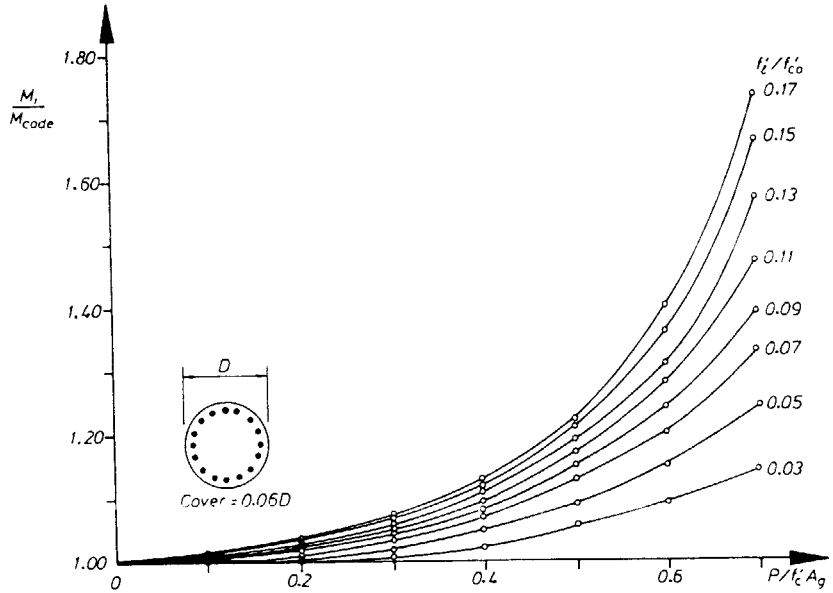

FIG. 15. Design Chart for Flexural-Strength Enhancement Factor for Circular Reinforced Concrete-Column Sections

concrete confinement, but neglecting the effect of steel strain hardening; and M_{code} = flexural strength of the section calculated using the conventional approach of ACI 318-89 and NZS 3101 assuming that the material strengths are as specified and that the strength reduction factor ϕ is unity. The same dimensionless parameters for confining stress f_l'/f_{co}' and axial-load level $P/f_c'A_g$ are used as in Fig. 14. It is evident in Fig. 15 that for axial-load levels $P/f_c'A_g$ of less than about 0.3, the enhancement of the flexural strength due to concrete confinement is relatively small, but that for higher axial-load levels, the enhancement of flexural strength due to concrete confinement can be very high. For the calculation of the ideal flexural strength M_i, including the effect of both concrete confinement and steel strain hardening, an additional factor has to be applied to the M_i in Fig. 15 to allow for the strength enhancement due to strain hardening of the flexural steel. That factor is more or less independent of the axial-load ratio and can be taken as approximately 1.10.

The enhancement in flexural strength due to concrete confinement and steel strain hardening is currently neglected by code provisions for the design of column sections for flexure and axial load. The enhancement, at least for concrete confinement, could be taken advantage of in the design of the longitudinal reinforcement of columns, because it leads to a reduction in the required area of longitudinal reinforcement if the axial compressive load is substantial. The enhancement should be included in the calculation of the design shear forces corresponding to the development of plastic hinges in columns, so that the greatest likely shear force is obtained.

Design Procedure Based on Design Charts

Zahn et al. (1986a) have developed a comprehensive design procedure for the flexural strength and ductility of reinforced concrete bridge columns

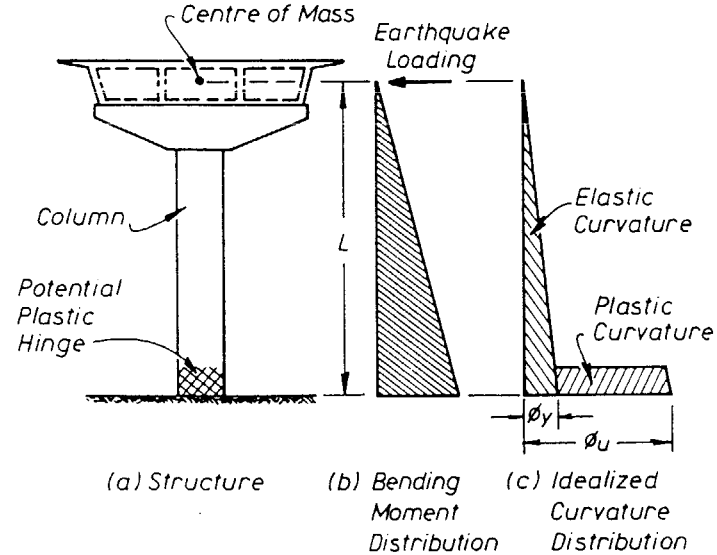

FIG. 16. Cantilever-Bridge Column with Lateral Earthquake Loading at Ultimate Lateral Displacement

based on the design charts. In the procedure, the designer chooses the level-of-displacement ductility factor and obtains the associated code-recommended–design seismic lateral loading for the bridge substructure. The required curvature-ductility factor at the plastic-hinge locations in the columns is then calculated from the geometry of the bridge substructure and the imposed displacement ductility factor. For example, for the cantilever-bridge column shown in Fig. 16, the relationship between the curvature-ductility factor ϕ_u/ϕ_y and the displacement ductility factor μ may be approximated (Priestley and Park, 1984, 1987) as

$$\frac{\phi_u}{\phi_y} = 1 + \frac{C(\mu - 1)}{3\frac{L_p}{L}\left(1 - 0.5\frac{L_p}{L}\right)} \tag{8}$$

where C = ratio of the elastic flexibility of the system due to the column, foundation, and bearings to the elastic flexibility due to the column alone; L = height of the center of mass of the bridge deck above the ground; and L_p = equivalent plastic-hinge length. Test data (Priestley and Park 1984, 1987) has shown that on average

$$L_p = 0.08L + 6d_b \tag{9}$$

where d_b = diameter of the longitudinal reinforcing bars. A good approximation for L_p is half of one column depth ($0.5D$ or $0.5h$).

Next, using the design charts for the curvature-ductility factor (e.g., Fig. 14), the required quantity of transverse reinforcement for confinement is obtained. Then the longitudinal reinforcement in the columns is calculated taking into account the enhancement in flexural strength of the column due to confinement (e.g., using Fig. 15). Finally, the transverse reinforcement is checked to ensure that it is adequate for the shear force assuming that

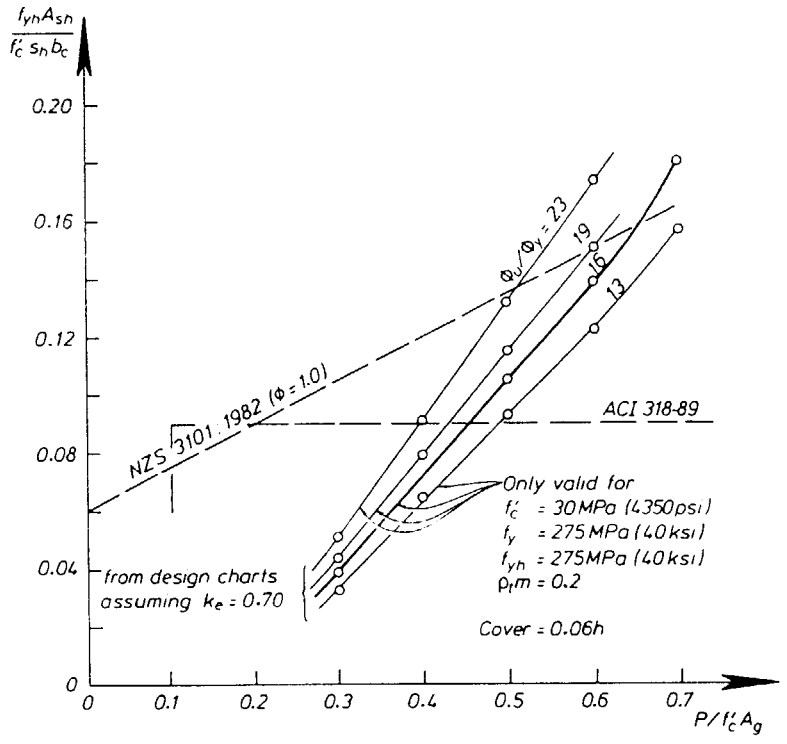

FIG. 17. Required Amount of Confining Steel for Ductility in Plastic-Hinge Region of Rectangular Column and Comparison with Requirements of NZS 3101 and ACI 318-89 for Ductile Frames

the plastic-hinge regions have developed their overstrength moment capacity, and that it is adequate to prevent premature buckling of the longitudinal reinforcement. These design steps may need to be repeated to obtain the final solution. This design procedure enables a more precise determination of the quantities of longitudinal and transverse reinforcement required in bridge columns for adequate strength and ductility.

Comparison of Ductility Charts with Code Equations

Fig. 17 shows a comparison of the quantities of transverse reinforcement required for the confinement of a typical rectangular column according to the ACI 318-89 and the NZS 3101 codes with the quantities found for various ϕ_u/ϕ_y values from the design charts. Although the comparison in Fig. 17 is for a particular column, it can be concluded that the quantities of transverse reinforcement determined using the design charts depends more significantly on the axial-load level P/f'_cA_g than the equations of the concrete design codes. While the equations of the codes are quite conservative for axial-load levels P/f'_cA_g less than about 0.4, they may be unconservative for higher axial-load levels, particularly when the quantity of flexural steel in the column is small. Also, it can be observed that the quantity of confining steel required depends on the flexural steel content, a factor that is not taken into account by the code equations. The U.S. code equations are independent of the axial-load level and as a result are very conservative at low axial-load levels and unconservative at high axial-load levels.

REFINED DESIGN EQUATIONS FOR CONFINING REINFORCEMENT

Approach and Parameters Investigated

Watson and Park (1989) have recently used the design charts of Zahn et al. (1986a) to obtain refined design equations for the quantities of confining reinforcement required in the potential plastic-hinge regions of columns.

The types of column sections investigated and reinforcement arrangements are shown in Fig. 18. The sections were of circular, square, and rectangular shape. The rectangular sections had an aspect ratio of 1.5 and bending about both axes was considered.

Table 2 lists the range of parameters investigated. It was considered that a range of curvature-ductility factors ϕ_u/ϕ_y from 10 to 20 should cover all likely cases of design for limited ductility and full ductility. Axial-load levels P/f'_cA_g less than 0.2 were not investigated, since, for lightly loaded columns, the role of transverse reinforcement for confinement of concrete is not as important as that of transverse reinforcement required both for lateral support of longitudinal bars to prevent premature buckling and for shear resistance. The ranges of concrete compressive strength f'_c, mechanical reinforcing ratio $\rho_t m$ and concrete-cover ratios c/h and c/D investigated represent values typically used in design, where c = cover thickness; h = dimension of a rectangular column in the direction of bending; and D = diameter of a circular column.

The yield strength of the reinforcement in the investigation was held constant at 275 MPa (40 ksi). It was shown in previous studies (see Zahn et al. 1986a) that changes in the yield strength of the longitudinal reinforcement within the normal range had an insignificant effect on the available curvature-ductility factor of columns providing that the shape of the stress-strain curves was similar. It was also shown (Zahn et al. 1986a) that the stress-strain curves for concrete confined by grades 380 [f_{yh} = 380 MPa (55 ksi)] and 275 [f_{yh} = 275 MPa (40 ksi)] transverse reinforcement are almost identical providing that the ratio of effective lateral confining stress to concrete strength f_l/f'_{co} and the transverse bar spacing s are similar. That is, variation of the yield strength of transverse reinforcement, but with yield

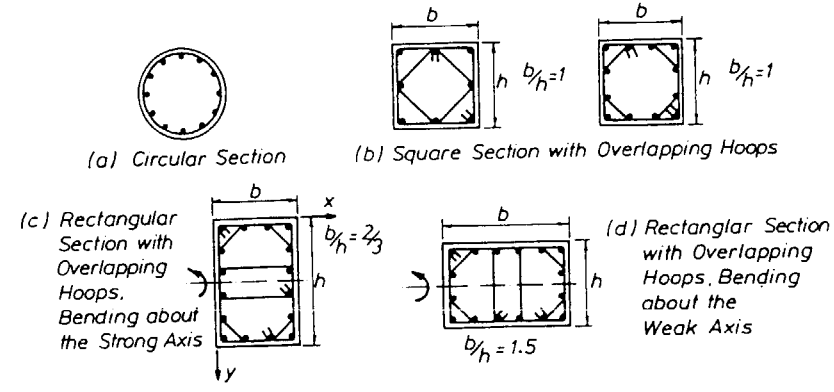

FIG. 18. Column Sections Investigated

TABLE 2. Range of Parameters Investigated in Development of Refined Design Equations

Parameter (1)	Range (2)
ϕ_u/ϕ_y	10–20
P/f'_cA_g	0.2–0.7
f'_c [MPa (psi)]	20–40 (2,900–5,800)
$\rho_t m$	0.1–0.4
c/h	0.02–0.08
c/D	0.06

force held constant by varying the bar diameter appropriately, does not change the effectiveness of the confinement.

Effective Lateral Confining Stress

For the circular section shown in Fig. 18(*a*) and referring to (1) and Fig. 2(*c*), the effective lateral confining stresses in each direction are

$$f'_l = k_e \frac{2A_b f_{yh}}{sd_c} \tag{10}$$

Noting that $\rho_s = 4A_b/sd_c$ and assuming that $k_e = 0.85$ and $f'_{co} = 0.85f'_c$ as suggested by Zahn et al. (1986a), (10) can be rewritten as

$$\rho_s \frac{f_{yh}}{f'_c} = \frac{2f'_l}{f'_{co}} \tag{11}$$

For the square section shown in Fig. 18(*b*) and referring to (1) and Fig. 2(*b*), the effective lateral confining stress in each direction is

$$f'_l = k_e \frac{3.41A_b f_{yh}}{sb_c} \tag{12}$$

Having $\rho_s = 3.41A_b/sb_c$ and assuming that $k_e = 0.7$ and $f'_{co} = 0.85f'_c$ as suggested by Zahn et al. (1986a), (12) may be rewritten as

$$\rho_s \frac{f_{yh}}{f'_c} = 1.214 \frac{f'_l}{f'_{co}} \tag{13}$$

For the rectangular section shown in Figs. 18(*c* and *d*), and referring to (1) and Figs. 2(*a* and *b*), the average effective lateral confining stress in the two directions x and y is

$$f'_l = 0.5(f'_{lx} + f'_{ly}) = k_e \rho_s f_{yh} \tag{14}$$

where $\rho_s = 0.5(\rho_{sx} + \rho_{sy})$, and where for Fig. 18(*c*) $\rho_{sx} = 5.41A_b/sh_c$ and $\rho_{sy} = 3.41A_b/sb_c$, and for Fig. 18(*d*) $\rho_{sx} = 3.41A_b/sh_c$ and $\rho_{sy} = 5.41A_b/sb_c$. If $k_e = 0.70$ and $f'_{co} = 0.85f'_c$, (14) can be rewritten as

$$\rho_s \frac{f_{yh}}{f'_c} = 1.25 \frac{f'_l}{f'_{co}} \tag{15}$$

Quantities of Confining Reinforcement

The quantities of transverse reinforcement required for the circular, square, and rectangular column sections shown in Fig. 18 were found from the f'_l/f'_{co} values obtained from the design charts for the range of values of the parameters listed in Table 2. The following conclusions concerning the influence of those parameters were reached by Watson and Park (1989).

The quantity of transverse reinforcement required for confinement for a particular curvature-ductility factor increases significantly when the axial-load ratio P/f'_cA_g increases. This is because when the axial-load ratio is high, the flexural strength of columns is more dependent on the concrete compressive strength and stress distribution. As a result, more transverse reinforcement is required to provide adequate confinement. Also, when the axial-load ratio is high the cyclic moment-curvature history used in the analysis (that is, four identical symmetrical cycles to the ultimate curvature) leads to greater strength deterioration of the concrete than in the case of monotonic loading.

The quantity of transverse reinforcement required for confinement increases when the longitudinal reinforcing ratio ρ_t decreases. This is because when ρ_t is small, the flexural strength of the column is more dependent on the concrete compressive strength and stress distribution.

The quantity of transverse reinforcement required for confinement increases when the concrete compressive strength increases. This is because concrete with a high compressive strength is more brittle.

The quantity of transverse reinforcement required for confinement increases when the concrete-cover thickness ratio c/D or c/h increases. This is because when c/D or c/h is high, the column loses significant flexural strength when the cover concrete spalls unless the concrete core is adequately confined.

The type of column section has a significant effect on the quantity of transverse reinforcement required for confinement. To achieve the same curvature-ductility factor, the quantity of transverse reinforcement required for circular sections is markedly different from the quantity of transverse reinforcement required for square and rectangular sections. However, the quantities of transverse reinforcement required for square and rectangular sections are not significantly different. This indicates that the square and rectangular sections investigated in the present study may represent the wide range of rectangular sections used in design.

Derivation of Equations

It is evident that refined design equations for the quantities of confining reinforcement required in columns need to be related to the required curvature-ductility factor ϕ_u/ϕ_y, and also to the examined parameters, namely P/f'_cA_g, f'_c, $\rho_t m$, c/D, or c/h, section type, and f_{yh}. For convenience, the influence of the relative cover thickness c/D or c/h is expressed by the ratio of A_g/A_c in the present study, where A_g is the gross area of the column section and A_c is the area of the concrete core.

Fig. 19 shows plots for $\rho_s f_{yh}/f'_c$ obtained by Watson and Park (1989) from the design charts for $\rho_t m = 0.1$–0.4, and for the range of other parameters listed in Table 2, to achieve curvature-ductility factors of either 20 or 10. The values of $\rho_s f_{yh}/f'_c$ for circular sections are larger than those for square and rectangular sections for the same values of $\rho_t m$, P/f'_cA_g, and c/D or c/h. It was decided therefore, to evaluate only the values of $\rho_s f_{yh}/f'_c$ for square and rectangular sections, and a section-type factor could then be

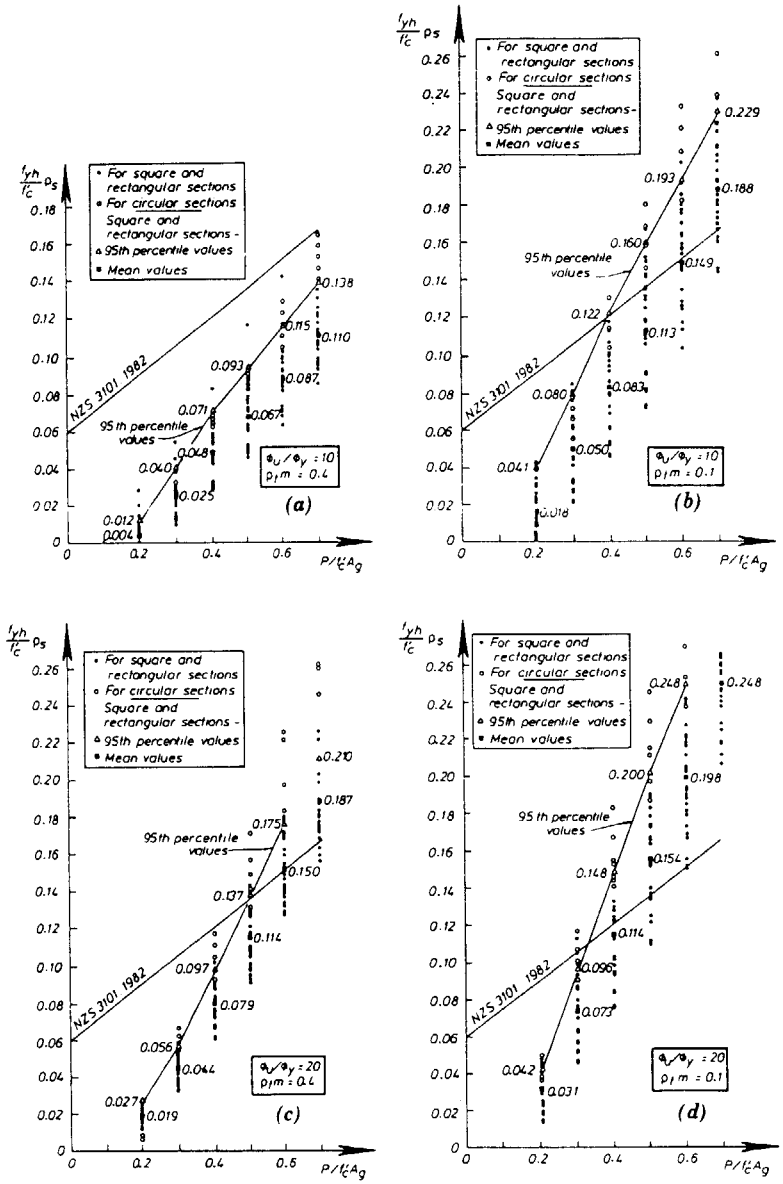

FIG. 19. Required Quantities of Confining Reinforcement in Potential Plastic-Hinge Regions of Columns Obtained from Design Charts to Achieve: (*a*) ϕ_u/ϕ_y = 10 with $\rho_t m$ = 0.4; (*b*) ϕ_u/ϕ_y = 10 with $\rho_t m$ = 0.1; (*c*) ϕ_u/ϕ_y = 20 with $\rho_t m$ = 0.4; and (*d*) ϕ_u/ϕ_y = 20 with $\rho_t m$ = 0.1.

applied to obtain the values of $\rho_s f_{yh}/f'_c$ for circular sections. Fig. 19 also shows a significant scatter. However, a suitable linear design equation was fitted to the results using the procedure to be described.

The 95th percentile and the mean values of $\rho_s f_{yh}/f'_c$ are shown plotted in

TABLE 3. Best Fit Equations for 95th Percentile Values of $\rho_s f_{yh}/f'_c$ for Square and Rectangular Columns

$\rho_t m$ (1)	ϕ_u/ϕ_y = 10 (2)	ϕ_u/ϕ_y = 15 (3)	ϕ_u/ϕ_y = 20 (4)
0.1	$y = 0.377x - 0.032$	$y = 0.426x - 0.039$	$y = 0.497x - 0.053$
0.2	$y = 0.336x - 0.036$	$y = 0.387x - 0.048$	$y = 0.465x - 0.059$
0.3	$y = 0.302x - 0.038$	$y = 0.333x - 0.046$	$y = 0.413x - 0.056$
0.4	$y = 0.252x - 0.035$	$y = 0.303x - 0.042$	$y = 0.372x - 0.050$

Note: $\rho_t m = \rho_t f_y/0.85f'_c$, $y = \rho_s f_{yh}/f'_c$, and $x = P/f'_c A_g$.

Fig. 19. Other 95th percentile values were calculated for the results, and the best fit linear equations of $\rho_s f_{yh}/f'_c$ as a function of $P/f'_c A_g$ for $\rho_t m$ = 0.1, 0.2, 0.3, and 0.4, and for ϕ_u/ϕ_y = 10, 15, and 20, were determined by the method of least squares. The values obtained are shown in Table 3, where $y = \rho_s f_{yh}/f'_c$; and $x = P/f'_c A_g$. The values for the coefficients in the equations in Table 3 were analyzed. Writing

$$\frac{\rho_s f_{yh}}{f'_c} = \frac{AP}{f'_c A_g} + B \tag{16}$$

it was found that for a wide range of cover ratios c/h the coefficients A and B could be represented with excellent accuracy by

$$A = \frac{A_g}{A_c}\left(-0.3\rho_t m + 0.009\frac{\phi_u}{\phi_y} + 0.208\right) \tag{17}$$

$$B = -1.4 \times 10^{-3}\left(\frac{\phi_u}{\phi_y}\right)^2 - 1.7 \times 10^{-2}\frac{\phi_u}{\phi_y} + 0.036 \tag{18}$$

By combining (16), (17), and (18), the following equation was derived by Watson and Park (1989) for square and rectangular columns:

$$\rho_s \frac{f_{yh}}{f'_c} = \frac{A_g}{A_c}\left(-0.3\rho_t m + 0.009\frac{\phi_u}{\phi_y} + 0.208\right)\frac{P}{f'_c A_g} - \left[1.40 \times 10^{-3}\left(\frac{\phi_u}{\phi_y}\right)^2 + 1.7 \times 10^{-2}\frac{\phi_u}{\phi_y} - 0.036\right] \tag{19}$$

Inspection of (19) indicates that the second term on the right-hand side is small compared to the first term and can be replaced by a numerical constant with good accuracy. Also, to use (19) for circular sections it was found that it needed to be multiplied by a section-type factor of 1.4.

Hence, the refined design equations for square, rectangular, and circular column sections can be written as follows for use in design with a strength reduction factor ϕ included in the axial-load ratio term.

For square or rectangular sections $\rho_s = A_{sh}/sb_c$, where A_{sh} = total effective area of transverse bars in direction under consideration; s = center-to-center spacing of rectangular hoops; and b_c = width of the concrete core measured perpendicular to the direction of the transverse reinforcement under consideration [see Fig. 2(*a* and *b*)]. Hence, from (19)

$$\frac{A_{sh}}{sb_c} = \frac{A_g}{A_c}\frac{\left(\frac{\phi_u}{\phi_y} - 33\rho_t m + 22\right)}{111}\frac{f'_c}{f_{yh}}\frac{P}{\phi f'_c A_g} - 0.006 \qquad (20)$$

For circular sections $\rho_s = 4A_b/sd_c$, where A_b = area of spiral or circular hoop bar; s = center-to-center spacing of spirals or circular hoops; and d_c = diameter of concrete core [see Fig. 2(c)]. Hence, from (19) and using a section type factor of 1.4

$$\frac{4A_b}{sd_c} = 1.4\frac{A_g}{A_c}\frac{\left(\frac{\phi_u}{\phi_y} - 33\rho_t m + 22\right)}{111}\frac{f'_c}{f_{yh}}\frac{P}{\phi f'_c A_g} - 0.008 \qquad (21)$$

The refined design equations, (20) for square and rectangular columns and (21) for circular columns, can be used either to determine the quantities of transverse reinforcement required to achieve specified curvature-ductility factors, or to determine the available curvature-ductility factors when the reinforcement is given.

Comparison with Current Code Equations

It is clear from Figs. 17 and 19 that, to achieve a curvature-ductility factor of $\phi_u/\phi_y = 20$, the current code equations for transverse reinforcement for concrete confinement result in more than sufficient confining reinforcement for columns with low to medium axial-load ratios, but result in insufficient confining reinforcement for columns with large axial-load ratios. It is evident that (20) and (21) can be used to achieve a better match of the available and required curvature-ductility factors than can be achieved with the current code equations. A curvature-ductility factor of $\phi_u/\phi_y = 20$ could be specified for ductile design and $\phi_u/\phi_y = 10$ for design for limited ductility in cases where a full calculation of the required curvature-ductility factor was unwarranted.

Although the refined equations are more complex than the current code equations, the advantage of more rational and precise design appears to outweigh this complexity. In any case, design charts can be drawn up to enable easier use of the refined equations. A further advantage is that in fact there is only one basic equation [the difference between (20) and (21) is a factor of 1.4]. Hence, the number of equations in the code is reduced.

CONCLUSIONS

Six major conclusions were reached in the analytical study of the flexural strength and ductility of reinforced concrete-column sections with various arrangements and quantities of transverse and longitudinal reinforcement.

Design charts for the available curvature-ductility factor can be derived using theoretical cyclic moment-curvature analyses incorporating cyclic stress-strain relationships for confined and unconfined concrete and for longitudinal reinforcing steel. The cyclic stress-strain curves for confined concrete take into account the quantity and arrangement of the transverse reinforcement and the accumulation of strain energy in the transverse reinforcement.

The quantity of transverse reinforcement required for confinement to achieve a curvature-ductility factor in the order of 15–20 is less than that

calculated using current code equations for axial-compression-load levels $P/f'_c A_g < 0.4$, but may be greater for $P/f'_c A_g > 0.4$.

The quantity of transverse reinforcement required for confinement to meet any particular curvature-ductility factor demand increases with increasing axial-load level, increasing concrete strength, decreasing longitudinal reinforcement ratio, and increasing relative cover-concrete thickness. Also, more transverse reinforcement is required for the confinement of square and rectangular columns than for circular columns.

Using linear regression analysis, refined design equations, (20) and (21), were obtained for the quantity of transverse reinforcement required for confinement.

The refined design equations give only the transverse reinforcement required for concrete confinement. The transverse reinforcement provided must also be checked to ensure that it is sufficient to prevent premature buckling of the longitudinal compression bars and to prevent shear failure. For low axial-load levels, the transverse reinforcement required for lateral restraint of longitudinal bars and for shear govern the design.

There is a significant increase in the flexural strength of columns due to confinement of the concrete by transverse reinforcement for axial-compression-load levels $P/f'_c A_g$ greater than about 0.3. This enhancement in flexural strength can be taken advantage of in the design of the longitudinal reinforcement and should be included in the calculation of the design shear forces corresponding to the development of plastic hinges in columns.

ACKNOWLEDGMENTS

The writers gratefully acknowledge the generous financial assistance of the University of Canterbury, the National Roads Board of New Zealand (now Transit New Zealand) and the New Zealand Ministry of Works and Development (now Works Consultancy Services).

APPENDIX I. REFERENCES

"Building code requirement for reinforced concrete and commentary." (1989). *ACI 318-89*, *ACI 318R-89*, American Concrete Institute (ACI), Detroit, Mich.

"Code of practice for the design of concrete structures; commentary on the design of concrete structures; amendment no. 1 to NZS 3101: parts 1 and 2." (1989). *NZS 3101 Part 1:1982*, *NZS 3101 Part 2:1982*, Standards Association of New Zealand, Wellington, New Zealand.

Mander, J. B., Priestley, M. J. N., and Park, R. (1984). "Seismic design of bridge piers." *Res. Rep. 84-2, Dept. of Civ. Engrg.*, Univ. of Canterbury, Christchurch, New Zealand.

Mander, J. B., Priestley, M. J. N., and Park, R. (1988a). "Observed stress-strain behavior of confined concrete." *J. Struct. Engrg.*, ASCE, 114(8), 1827–1849.

Mander, J. B., Priestley, M. J. N., and Park, R. (1988b). "Theoretical stress-strain model for confined concrete." *J. Struct. Engrg.*, ASCE, 114(8), 1804–1826.

Park, R., and Leslie, P. D. (1977). "Curvature ductility of circular reinforced concrete columns confined by the ACI spiral." *Proc., 6th Australasian Conf. on the Mech. of Struct. and Mat., Vol. 1*, Christchurch, New Zealand, 342–349.

Park, R., and Norton, J. A. (1974). "Effects of confining reinforcement on the flexural ductility of rectangular reinforced concrete column sections with high strength steel." *Symp. on Des. and Safety of Reinforced Concrete Compression Members, Reps. of Working Commissions, Vol. 16*, International Association for Bridge and Structural Engineering, Quebec, Canada, 267–275.

Park, R., and Paulay, T. (1975). "Reinforced concrete structures." John Wiley & Sons, New York, N.Y.
Park, R., and Paulay, T. (1990). "Strength and ductility of concrete substructures of bridges." *RRU Bull. No. 84, Vol. 1*, Road Res. Unit, Transit New Zealand, Wellington, New Zealand.
Park, R., and Sampson, R. A. (1972). "Ductility of reinforced concrete column sections in seismic design." *J. Am. Concrete Inst.*, 69(9), 543–551.
Priestley, M. J. N., and Park, R. (1984). "Strength and ductility of bridge substructures." *RRU Bull. No. 71*, Road Res. Unit, Nat. Roads Board, Wellington, New Zealand.
Priestley, M. J. N., and Park, R. (1987). "Strength and ductility of concrete bridge columns under seismic loading." *Struct. J. Am. Concrete Inst.*, 84(1), 61–76.
"Recommended Lateral Force Requirements and Commentary." (1975). Structural Engineers Association of California, San Francisco, Calif.
Watson, S., and Park, R. (1989). "Design of reinforced concrete frames of limited ductility." *Res. Rep. 89-4*, Dept. of Civ. Engrg., Univ. of Canterbury, Christchurch, New Zealand.
Zahn, F. A., Park, R., and Priestley, M. J. N. (1986a). "Design of reinforced concrete bridge columns for strength and ductility." *Res. Rep. 86-7*, Dept. of Civ. Engrg., Univ. of Canterbury, Christchurch, New Zealand.
Zahn, F. A., Park, R., Priestley, M. J. N., and Chapman, H. E. (1986b). "Development of design procedures for the flexural strength and ductility of reinforced concrete bridge columns." *Bull. of the New Zealand Nat. Soc. for Earthquake Engrg.*, 19(3), 200–212.

APPENDIX II. NOTATION

The following symbols are used in this paper:

A_b = area of spiral or circular hoop bar, or longitudinal bar;
A_c = area of concrete core of column section measured to outside of peripheral spiral or hoop;
A_g = gross area of column section;
A_{sh} = total effective area of transverse bars in direction under consideration within spacing s;
b_c = width of concrete core of column section measured perpendicular to direction of transverse bars under consideration to center of peripheral hoop;
C = coefficient representing increase in elastic flexibility of system due to foundations and bearings;
c = thickness of concrete cover;
D = diameter of circular column;
d_b = bar diameter;
d_c = diameter of concrete core of column section measured to center of peripheral circular hoop or spiral;
E_c = modulus of elasticity of concrete;
E_r = reduced modulus of steel;
E_{sh} = strain-hardening modulus of steel;
f_c = longitudinal stress in concrete;
f'_c = compressive cylinder strength of concrete;
f'_{cc} = peak longitudinal compressive stress of stress-strain curve of confined concrete;
f'_{co} = peak longitudinal compressive stress of stress-strain curve of unconfined concrete;
f_l = lateral confining stress acting on concrete;

f'_l = effective lateral confining stress acting on concrete;
f'_{lx} = effective lateral confining stress acting on concrete in x direction;
f'_{ly} = effective lateral confining stress acting on concrete in y direction;
f_s = stress in steel;
f_{su} = ultimate tensile strength of steel;
f_{suc} = compressive stress in longitudinal steel bar at buckling;
f'_t = modulus of rupture of concrete;
f_y = yield strength of longitudinal steel reinforcement;
f_{yh} = yield strength of transverse steel reinforcement;
h = lateral dimension of rectangular column section;
h_c = width of core of column section measured perpendicular to direction of transverse bars under consideration to center of peripheral hoop;
k_e = confinement effectiveness coefficient;
L = height of column to center of mass;
L_p = equivalent plastic-hinge length;
M_{code} = flexural strength calculated by ACI 318-89 or NZS 3101, but using measured material strengths and assuming $\phi = 1$;
M_i = ideal flexural strength;
M_{max} = maximum moment;
M'_y = moment when yield is first reached in longitudinal reinforcement or when extreme fiber concrete compressive strain reaches 0.002, whichever occurs first;
m = $f_y/0.85f'_c$;
P = compressive load on column, or strain-hardening power;
R = experimentally calibrated factor;
s = center-to-center spacing of spirals or hoops;
ε_c = longitudinal compression strain in concrete;
ε_{cc} = longitudinal compression strain in confined concrete corresponding to f'_{cc};
ε_{co} = longitudinal compression strain in unconfined concrete corresponding to f'_{co};
ε_{cu} = ultimate longitudinal compressive strain of confined concrete;
ε_s = strain in steel, or strain in reinforcement located nearest extreme tension fiber;
ε_{sh} = steel strain at commencement of strain hardening;
ε_{sp} = compressive strain in unconfined concrete when spalling occurs and longitudinal concrete stress there is reduced to zero;
ε_{su} = steel strain corresponding to f_{su};
ε_{suc} = compressive strain in longitudinal steel bar at buckling;
μ = displacement ductility factor; ratio of maximum or ultimate displacement Δ_u to yield displacement Δ_y, both measured at center of mass of bridge superstructure;
ρ_s = ratio of volume of transverse reinforcement to volume of concrete core;
ρ_{sx} = volumetric ratio of effective confining reinforcement in x direction;
ρ_{sy} = volumetric ratio of effective confining reinforcement in y direction;
ρ_t = area of longitudinal column steel divided by gross area of column section;

ϕ = strength-reduction factor, or curvature;
ϕ_{peak} = peak curvature;
ϕ_u = ultimate or maximum curvature;
ϕ_y = yield curvature; and
ϕ_y' = curvature when yield is first reached in longitudinal reinforcement or when extreme concrete fiber compressive strain reaches 0.002, whichever occurs first.